



Recurrence and non-improvement of European Heart Rhythm Association symptom scores after atrial fibrillation ablation: the role of left atrial fractal dimension

Mengyuan Jing^{1,2,3,4#}, Qing Liu^{1,2,3,4#}, Huaze Xi^{1,2,3,4#}, Xingmei Yang^{1,2,3,4}, Hao Zhu^{1,2,3,4}, Qiu Sun^{1,2,3,4}, Gang Chen⁵, Yuting Zhang^{1,2,3,4}, Wei Ren⁶, Liangna Deng^{1,2,3,4}, Tao Han^{1,2,3,4}, Bin Zhang^{1,2,3,4}, Junlin Zhou^{1,2,3,4}

¹Department of Radiology, Lanzhou University Second Hospital, Lanzhou, China; ²Second Clinical School, Lanzhou University, Lanzhou, China; ³Key Laboratory of Medical Imaging of Gansu Province, Lanzhou, China; ⁴Gansu International Scientific and Technological Cooperation Base of Medical Imaging Artificial Intelligence, Lanzhou, China; ⁵Cardiac Care Unit, Department of Cardiovascular Medicine, Lanzhou University Second Hospital, Lanzhou, China; ⁶GE Healthcare, Computed Tomography Research Center, Beijing, China

Contributions: (I) Conception and design: M Jing, Q Liu, H Xi; (II) Administrative support: J Zhou; (III) Provision of study materials or patients: M Jing, Q Liu, H Xi, X Yang, H Zhu, Q Sun, G Chen, Y Zhang; (IV) Collection and assembly of data: H Zhu, Q Sun, G Chen, Y Zhang; (V) Data analysis and interpretation: M Jing, Q Liu, H Xi, W Ren; (VI) Manuscript writing: All authors; (VII) Final approval of manuscript: All authors.

#These authors contributed equally to this work.

Correspondence to: Junlin Zhou, MD, PhD. Department of Radiology, Lanzhou University Second Hospital, Cuiyingmen No. 82, Chengguan District, Lanzhou 730030, China; Second Clinical School, Lanzhou University, Lanzhou, China; Key Laboratory of Medical Imaging of Gansu Province, Lanzhou, China; Gansu International Scientific and Technological Cooperation Base of Medical Imaging Artificial Intelligence, Lanzhou, China. Email: ery_zhoujl@lzu.edu.cn.

Background: Atrial fibrillation (AF) is the most common sustained cardiac arrhythmia. Atrial remodeling often leads to impaired clinical outcomes after AF ablation. Understanding the factors influencing AF recurrence after ablation is crucial for improving patient prognosis. This study aimed to investigate the relationship between left atrial (LA) morphologic heterogeneity, quantified by fractal dimension (FD), and AF recurrence, as well as the impact on European Heart Rhythm Association (EHRA) symptom scores following ablation.

Methods: This study retrospectively collected the data of patients with AF who underwent their first radiofrequency ablation procedure at Lanzhou University Second Hospital between October 2019 and September 2022 and underwent cardiac computed tomography angiography (CTA) within 3 days before the procedure. Patients with less than 1 year of follow-up or those who did not meet the inclusion criteria were excluded from the analysis. On the cardiac CTA images, we calculated the FD of each patient's LA using fractal analysis. Cox proportional risk models were used to calculate the risk ratios for predictors of AF recurrence and for predictors of EHRA symptom score non-improvement.

Results: A total of 512 patients with AF were included with a median follow-up of 29 (range, 18–37) months, of which 349 had paroxysmal AF and 163 had persistent AF, 341 were male and 171 were female, 146 had recurrence of AF and 366 did not have recurrence, and 48 had improvement of EHRA symptoms and 98 did not have improvement. Cox regression analysis showed that LA-FD was an independent predictor of recurrence [hazard ratio (HR) =16.056, 95% confidence interval (CI): 7.493–34.406, $P<0.001$] and non-improvement in EHRA symptom score (HR =10.500, 95% CI: 3.086–35.728, $P<0.001$) after AF ablation. In patients with paroxysmal and persistent AF, LA-FD (HR =21.750, 95% CI: 8.533–55.444, $P<0.001$; HR =7.291, 95% CI: 1.977–26.896, $P<0.05$) is also an independent predictor of recurrence after AF ablation. Furthermore, patients with a larger LA-FD (>1.208) had a higher incidence of AF recurrence and EHRA

symptom score non-improvement than those with a smaller LA-FD (<1.208 , $P<0.05$).

Conclusions: A larger LA-FD (>1.208) on cardiac CTA could be a predictor for adverse LA remodeling and was independently associated with recurrence and non-improvement of the EHRA symptom score after AF ablation.

Keywords: Atrial fibrillation (AF); recurrence; European Heart Rhythm Association symptom scores (EHRA symptom scores); fractal dimension (FD); left atrial morphology (LA morphology)

Submitted Sep 24, 2024. Accepted for publication Feb 26, 2025. Published online Mar 28, 2025.

doi: 10.21037/qims-24-2049

View this article at: <https://dx.doi.org/10.21037/qims-24-2049>

Introduction

Atrial fibrillation (AF) is the most common cardiac arrhythmia, affecting millions of individuals worldwide, with a high clinical prevalence and significant disease burden (1,2). Compared with antiarrhythmic drugs, radiofrequency ablation is a commonly used treatment that can restore sinus rhythm and improve symptoms in certain patients with AF. However, its efficacy in preventing recurrence varies, and it may not significantly reduce cardiovascular mortality in all patient populations (3,4). The recurrence of postoperative AF and potential complications of ablation warrant careful patient selection to avoid unnecessary surgical risks and additional financial burdens. The European Heart Rhythm Association (EHRA) symptom score is a widely used clinical tool to assess the severity of AF-related symptoms, ranging from class I (no symptoms) to class IV (severe symptoms affecting daily activity), which allows for grading of patients with AF (5). In patients with AF, preoperative prediction of non-improvement in EHRA symptom scores may help identify patients who are less likely to experience significant symptom relief following ablation, guiding more personalized treatment decisions.

Previous studies have reported that greater left atrial (LA) wall thickness, increased diameter, larger volume and volume index, as well as more spherical LA morphology and box surface ratio, are associated with a higher risk of late AF recurrence following ablation (6-9). This suggests that, in addition to LA size, LA morphology can also indicate poor LA remodeling associated with recurrence after ablation.

To quantitatively describe the morphology of the LA, a mathematical method called fractal analysis was introduced. Fractal dimensions (FD) acquired based on fractal analysis can be applied to quantify shape complexity and boundary irregularity, capturing early morphologic changes that might precede volumetric alterations (10,11). We hypothesized

that LA-FD could serve as a novel biomarker to quantify adverse structural remodeling and be correlated with poor outcomes in patients with AF. Therefore, we quantified LA morphological heterogeneity using FD from cardiac computed tomography angiography (CTA) images, with the aim of investigating the relationship between LA-FD, AF recurrence, and changes in EHRA symptom scores after recurrence. Understanding these relationships could help guide personalized treatment strategies for patients undergoing ablation. We present this article in accordance with the STROBE reporting checklist (available at <https://qims.amegroups.com/article/view/10.21037/qims-24-2049/rc>).

Methods

Study population

This study was conducted in accordance with the Declaration of Helsinki (as revised in 2013). The study protocol was approved by the Institutional Review Board of Lanzhou University Second Hospital (ethical board approval number: 2023A-702). The informed consent was exempted for all individual patients because of the retrospective nature of the study.

We queried the information management system of Lanzhou University Second Hospital to identify 535 patients who underwent their first radiofrequency ablation procedure for paroxysmal or persistent AF and had CTA performed within three days before the procedure from October 2019 to September 2022. We routinely followed up our patients consecutively after ablation. We excluded patients based on the following criteria: age <18 years ($n=2$); follow-up time of less than 1 year ($n=3$); incomplete clinical and imaging data ($n=1$); with stent placement, bypass, or pacemaker ($n=5$); underwent valve replacement, left atrial

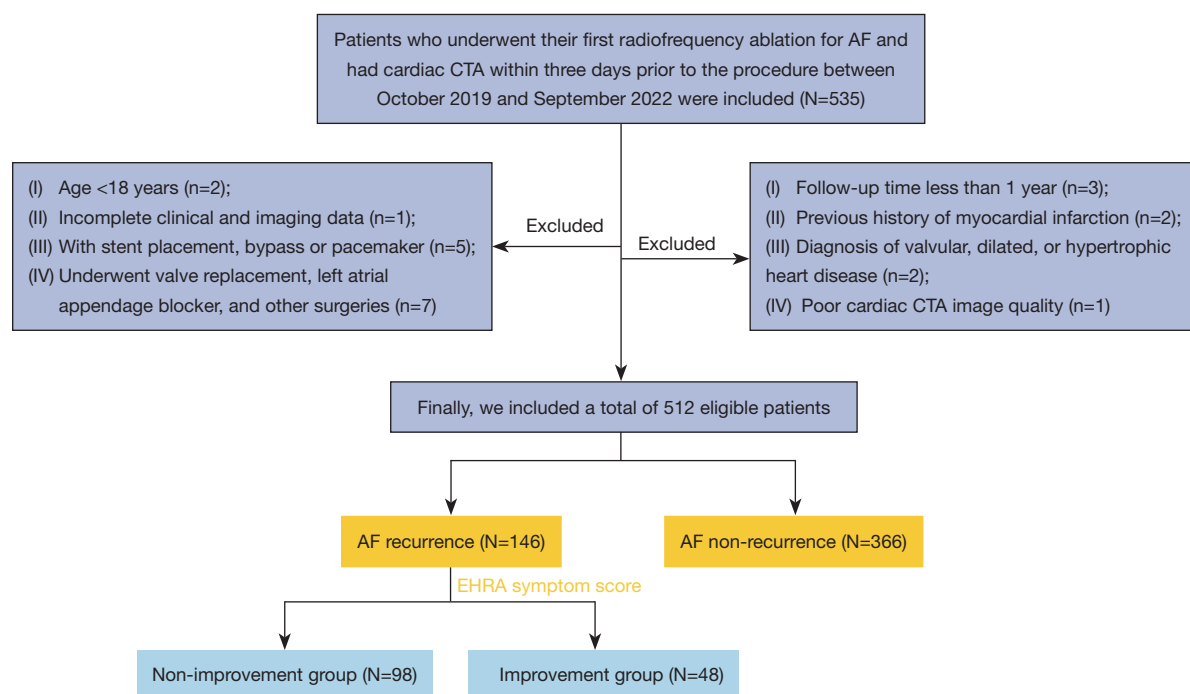


Figure 1 Patient screening flow chart. AF, atrial fibrillation; CTA, computed tomography angiography; EHRA, European Heart Rhythm Association.

appendage blocker, and other cardiac surgeries (n=7); previous history of myocardial infarction (n=2); diagnosis of valvular, dilated, or hypertrophic heart disease (n=2); and poor cardiac CTA image quality (n=1). Finally, 512 eligible patients were included in the study. *Figure 1* shows the patient enrollment process.

Cardiac CTA examination

After patients were admitted to the Lanzhou University Second Hospital, routine contrast-enhanced cardiac CTA was performed using three different computed tomography (CT) machines with a similar scanning protocol: Revolution 256-row CT (GE HealthCare, Waukesha, WI, USA), iCT 256 (Brilliance iCT256, Philips Healthcare, Netherlands), and dual-source Force CT (Somatom Force, Siemens Healthcare, Forchheim, Germany). [Table S1](#) provides more detailed information on the specific acquisition parameters used.

Radiofrequency ablation and postoperative follow-up

All enrolled patients with AF underwent ablation based on circumferential pulmonary vein isolation. The four pulmonary veins were isolated and observed for 30 min

to verify the bidirectional block between the left atrium and pulmonary veins. The patients were monitored using a 12-lead electrocardiogram and 24-hour ambulatory electrocardiogram every 3 months during the first year of the postoperative period and every 6 months thereafter at follow-up visits. When patients were not followed up as planned, they were followed up by telephone. The follow-up end point was AF recurrence or termination by December 2023. AF recurrence was defined as the detection of any atrial tachyarrhythmia (including atrial tachycardia, atrial flutter, and AF) lasting >30 seconds after a 3-month postoperative blanking period.

According to the European Society of Cardiology guidelines (5), cardiologists routinely evaluate the EHRA symptom scores preoperatively. In addition, patients with AF recurrence were assessed for changes in EHRA symptoms compared with the preoperative period. The EHRA symptoms that remained unchanged/worsened were considered the non-improvement group, and the EHRA symptoms that improved were considered the improvement group.

LA-FD measurement

The FD is measured by the box-counting method with the

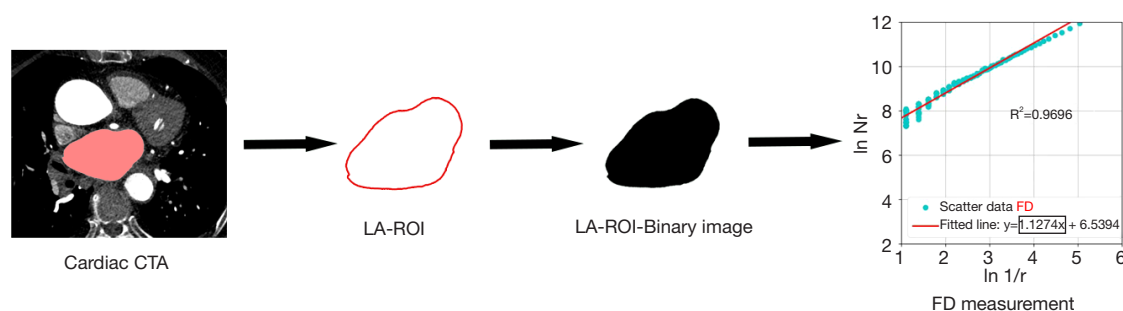


Figure 2 Schematic diagram of the measurement of the LA-FD. CTA, computed tomography angiography; FD, fractal dimension; LA, left atrial; ROI, region of interest.

formula (12):

$$d_f = -\lim_{\epsilon \rightarrow 0} \frac{\log(N(\epsilon))}{\log(\epsilon)} \quad [1]$$

First, the maximal level of the LA was determined on cardiac-enhanced CTA images by two radiologists with 10 years of experience in cardiovascular diagnosis (readers 1 and 2), neither of whom was aware of the patient's follow-up. Second, three-dimensional (3D) Slicer (version 5.2.0; USA) was used by reader 1 to outline three regions of interest (ROIs) along the outer edge of the LA, including the maximal level of the LA and its adjacent upper and lower layers. Furthermore, reader 2 checked the ROIs sketched by reader 1, and if there were ambiguities, they were negotiated and manually modified. Finally, Python 3.11 (<https://www.python.org>) was applied by reader 1 to calculate the FD of the three ROIs mentioned above. The average was taken to get the final FD. *Figure 2* shows a schematic diagram of the LA-FD measurements. The diameter, circumference, and square of the LA were measured three times at the maximal level using the Advanced Workstation 4.7 (GE Healthcare Waukesha, WI, USA) workstation by reader 1. The final result was determined by averaging the three measurements.

Statistical analysis

Statistical analyses were conducted with SPSS 26.0 (IBM Corp., Armonk, NY, USA). The frequencies (percentages) were utilized to express categorical variables. Continuous variables were shown as mean \pm standard deviation or median (interquartile range). Continuous variables were dichotomized according to mean values, and the Kaplan-Meier method was used to construct non-recurrence and EHRA symptom improvement survival curves. The log-

rank test was used to detect the difference between the survival distributions of the two curves. Survival analyses were performed using Cox proportional risk models to determine the risk ratios of single and multifactorial predictors of AF recurrence and EHRA symptom score improvement. A P value of <0.05 was considered statistically significant.

Results

Study population

Among 512 total patients, 349 (68.2%) patients had paroxysmal AF, 163 (31.8%) patients had persistent AF, 341 (66.6%) were males, 171 (33.4%) were females, and the median age was 59 [interquartile range (IQR), 52–67] years. During a median follow-up time of 29 (IQR, 18–37) months, 146 (28.5%) patients had a recurrence. In addition, the median LA-FD of the patients was 1.2087 (1.0766, 1.3227). *Table 1* shows the baseline characteristics of the study population.

Cox regression analysis for AF recurrence

In the univariate analysis, LA-FD [hazard ratio (HR) = 18.205, 95% confidence interval (CI): 8.599–38.544, $P < 0.001$] was a significant predictor of recurrence after ablation in all patients with AF, similar to current smoking (HR = 1.731, 95% CI: 1.132–2.647, $P = 0.011$) and the type of AF (HR = 0.576, 95% CI: 0.415–0.798, $P = 0.001$). Recurrence of AF was not predicted by any other clinical parameters such as age or sex ($P > 0.05$, *Table 2*). When meaningful univariate values were included in the multivariate analysis ($P < 0.05$), the LA-FD retained its predictive value for AF recurrence (HR = 16.056, 95% CI: 7.493, 34.406, $P < 0.001$; *Table 2*).

Table 1 Baseline characteristics of the study population (n=512)

Parameters	Value
Age (years)	59.00 (52.00, 67.00)
Gender	
Female	171 (33.4)
Male	341 (66.6)
BMI (kg/m ²)	24.57 (22.49, 26.71)
Current smoking	133 (26.0)
Drinking	84 (16.4)
Hypertension	238 (46.5)
Hyperglycaemia	159 (31.1)
Hyperlipidemia	286 (55.9)
Urea (mmol/L)	6.31 (5.30, 7.70)
CREA (μmol/L)	74.00 (64.00, 84.08)
Urea/CREA	0.09 (0.07, 0.11)
UA (μmol/L)	342.50 (283.00, 398.00)
COPD	180 (35.2)
TIA/stroke/embolism	154 (30.1)
Type of AF	
Paroxysmal	349 (68.2)
Persistent	163 (31.8)
CHA ₂ DS ₂ -VaSc score	2.00 (1.00, 3.00)
EHRA classification	
EHRA 1	36 (7.0)
EHRA 2a	181 (35.4)
EHRA 2b	208 (40.6)
EHRA 3	87 (17.0)

Table 1 (continued)**Table 1** (continued)

Parameters	Value
WBC (10 ⁹ /L)	6.15 (5.24, 7.40)
NE (10 ⁹ /L)	3.80 (3.08, 4.86)
LY (10 ⁹ /L)	1.64 (1.28, 2.02)
MO (10 ⁹ /L)	0.42 (0.35, 0.54)
PLT (10 ⁹ /L)	179.50 (138.25, 219.75)
NLR	2.32 (1.74, 3.18)
PLR	107.33 (84.63, 136.90)
LMR	3.76 (2.91, 4.83)
SII	402.87 (289.75, 600.04)
CAD	206 (40.2)
LA diameter (mm)	37.45 (33.20, 42.00)
LA circumference (mm)	284.55 (253.80, 312.93)
LA square (mm ²)	2,729.00 (2,179.48, 3,351.55)
LA-FD	1.2087 (1.0766, 1.3227)
AF recurrence	146 (28.5)
Follow-up time (months)	29.00 (18.00, 37.00)

Data are presented as median (IQR) or n (%). AF, atrial fibrillation; BMI, body mass index; CREA, creatinine; COPD, chronic obstructive pulmonary disease; CAD, coronary artery disease; EHRA, European Heart Rhythm Association; FD, fractal dimension; IQR, interquartile range; LY, lymphocyte count; LMR, lymphocyte-to-monocyte ratio; LA, left atrium; MO, monocyte count; NE, neutrophil count; NLR, neutrophil-to-lymphocyte ratio; PLT, platelet count; PLR, platelet-to-lymphocyte ratio; SII, systemic immune-inflammation index [(neutrophil count × platelet count)/lymphocyte count]; TIA, transient ischemic attack; UA, uric acid; WBC, white blood cell count.

Kaplan-Meier survival curves revealed a lower incidence of AF recurrence in patients with a small LA-FD (<1.208) than in those with a large LA-FD (>1.208) (*Figure 3A*).

Cox regression analysis for AF recurrence in patients with paroxysmal AF

In univariate Cox regression analysis, gender (HR =1.595, 95% CI: 1.022–2.490, P=0.040), current smoking (HR

=2.213, 95% CI: 1.197–4.089, P=0.011), uric acid level (HR =0.997, 95% CI: 0.995–1.000, P=0.041), and LA-FD (HR =24.310, 95% CI: 9.740–60.671, P<0.001) were predictors of recurrence in patients with paroxysmal AF; other clinical indicators did not predict recurrence in patients with paroxysmal AF (P>0.05), as shown in *Table 3*. The indicators with P<0.05 in the univariate analysis were included in the multivariate Cox regression analysis, and the results showed that LA-FD (HR 21.750, 95% CI: 8.533–55.444, P<0.001) was a predictor of recurrence in patients with paroxysmal AF (*Table 3*). The Kaplan-Meier survival curves showed a low incidence of AF recurrence in patients with paroxysmal

Table 2 Cox regression analysis for AF recurrence

Parameters	Univariate Cox regression		Multivariate Cox regression	
	HR (95% CI)	P value	HR (95% CI)	P value
Age (years)	1.000 (0.985, 1.015)	0.967		
Gender (male)	1.210 (0.863, 1.698)	0.269		
BMI (kg/m ²)	1.009 (0.967, 1.053)	0.680		
Current smoking	1.731 (1.132, 2.647)	0.011	0.620 (0.405, 0.949)	0.028
Drinking	1.320 (0.815, 2.138)	0.260		
Hypertension	1.022 (0.738, 1.415)	0.897		
Hyperglycaemia	0.777 (0.550, 1.098)	0.152		
Hyperlipidemia	0.915 (0.659, 1.270)	0.595		
Urea (mmol/L)	0.977 (0.903, 1.057)	0.562		
CREA (μmol/L)	1.002 (0.996, 1.008)	0.511		
Urea/CREA	0.733 (0.144, 3.732)	0.709		
UA (μmol/L)	0.999 (0.997, 1.001)	0.320		
COPD	0.942 (0.672, 1.321)	0.730		
TIA/stroke/embolism	0.747 (0.529, 1.056)	0.098		
Type of AF	0.576 (0.415, 0.798)	0.001	0.609 (0.439, 0.844)	0.003
CHA ₂ DS ₂ -VaSc score	1.078 (0.970, 1.199)	0.162		
EHRA classification				
EHRA 1	0.731 (0.426, 1.254)	0.255		
EHRA 2a	1.024 (0.762, 1.377)	0.873		
EHRA 2b	1.222 (0.922, 1.621)	0.163		
EHRA 3	0 (Ref)			
WBC (10 ⁹ /L)	0.970 (0.896, 1.051)	0.458		
NE (10 ⁹ /L)	0.968 (0.888, 1.056)	0.467		
LY (10 ⁹ /L)	0.934 (0.704, 1.241)	0.639		
MO (10 ⁹ /L)	1.163 (0.488, 2.772)	0.734		
PLT (10 ⁹ /L)	1.000 (0.997, 1.003)	0.995		
NLR	0.984 (0.924, 1.049)	0.626		
PLR	1.000 (0.998, 1.002)	0.809		
LMR	0.964 (0.872, 1.065)	0.467		
SII	1.000 (1.000, 1.000)	0.597		
CAD	1.201 (0.858, 1.680)	0.285		
LA diameter (mm)	1.004 (0.981, 1.027)	0.753		
LA circumference (mm)	0.998 (0.995, 1.002)	0.364		
LA square (mm ²)	1.000 (1.000, 1.000)	0.753		
LA-FD	18.205 (8.599, 38.544)	<0.001	16.056 (7.493, 34.406)	<0.001

AF, atrial fibrillation; BMI, body mass index; CI, confidence interval; CREA, creatinine; COPD, chronic obstructive pulmonary disease; CAD, coronary artery disease; EHRA, European Heart Rhythm Association; FD, fractal dimension; HR, hazard ratio; LY, lymphocyte count; LMR, lymphocyte-to-monocyte ratio; LA, left atrium; MO, monocyte count; NE, neutrophil count; NLR, neutrophil-to-lymphocyte ratio; PLT, platelet count; PLR, platelet-to-lymphocyte ratio; SII, systemic immune-inflammation index [(neutrophil count × platelet count)/lymphocyte count]; TIA, transient ischemic attack; UA, uric acid; WBC, white blood cell count.

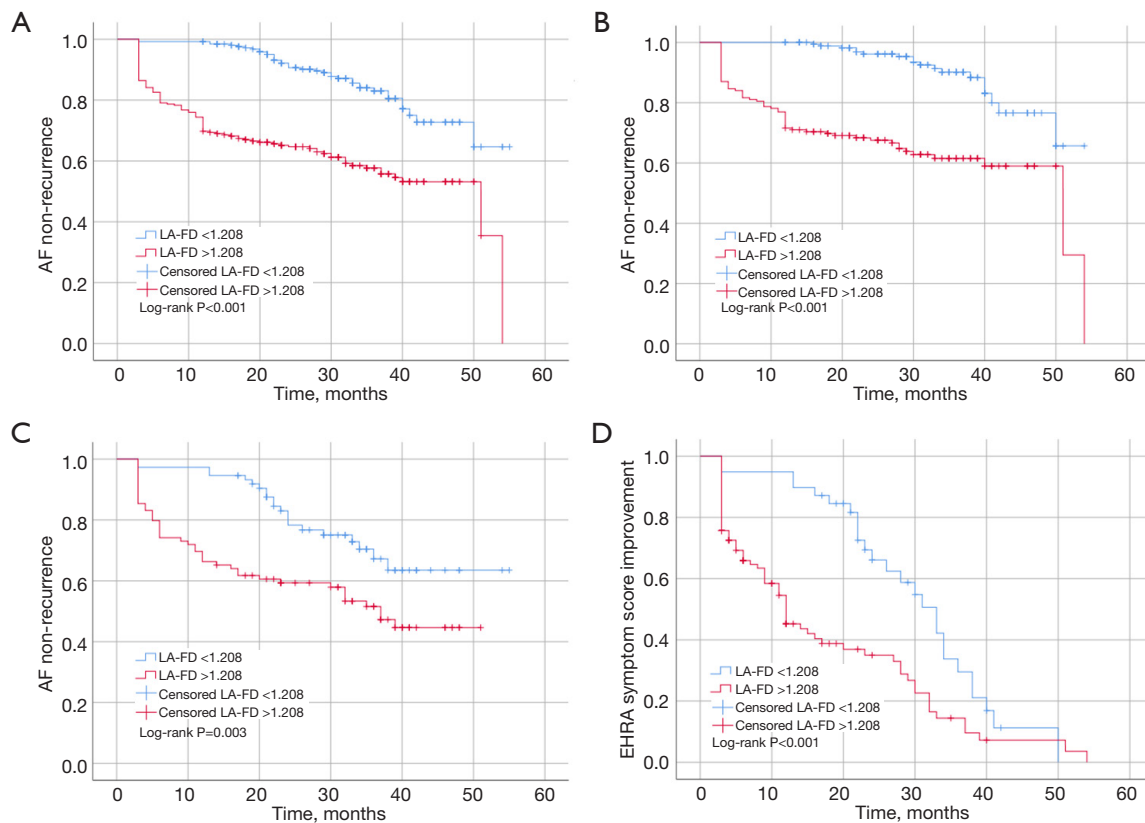


Figure 3 Kaplan-Meier curve for AF non-recurrence in all patients (A), in paroxysmal AF (B), in persistent AF (C), and for EHRA symptom score improvement (D). AF, atrial fibrillation; EHRA, European Heart Rhythm Association; FD, fractal dimension; LA, left atrial.

AF who had a small LA-FD (<1.208) (Figure 3B).

Cox regression analysis for AF recurrence in patients with persistent AF

Based on univariate analysis, only transient cerebral ischemic attacks/stroke/embolism (HR =0.550, 95% CI: 0.335–0.903, P=0.018) and LA-FD (HR =8.454, 95% CI: 2.316–30.864, P=0.001) were found to be predictors of recurrence in patients with persistent AF among the baseline characteristics of the patients. In addition, based on multivariate analysis, LA-FD (HR =7.291, 95% CI: 1.977–26.896, P=0.003) maintained its predictive value for the recurrence of persistent AF. The results are summarized in Table 4. Kaplan-Meier survival curves indicated a higher rate of AF recurrence in patients with persistent AF who had a larger LA-FD (>1.208) (Figure 3C).

Cox regression analysis for EHRA symptom score non-improvement

Among 146 patients with recurrent AF, median age was 59.53±0.88 years, 93 (63.7%) were males and 53 (36.3%) were females, 81 (55.5%) were patients with paroxysmal AF and 65 (44.5%) were patients with persistent AF. Compared to the preoperative EHRA symptom scores, 48 (32.9%) patients showed improvement and 98 (67.1%) showed no improvement.

The results of univariate Cox regression analysis showed that in addition to hyperlipidemia (HR =0.629, 95% CI: 0.416–0.952, P=0.028), lymphocyte count (HR =1.484, 95% CI: 1.097–2.007, P=0.010), platelet count (HR =1.003, 95% CI: 1.001–1.006, P=0.013), and neutrophil-to-lymphocyte ratio (HR =0.910, 95% CI: 0.836–0.990, P=0.029), LA-FD (HR =7.555, 95% CI: 2.347–24.323, P=0.001) was also a predictor of non-improvement in EHRA symptom scores.

Table 3 Cox regression analysis for AF recurrence in patients with paroxysmal AF

Parameters	Univariate Cox regression		Multivariate Cox regression	
	HR (95% CI)	P value	HR (95% CI)	P value
Age (years)	1.004 (0.984, 1.025)	0.679		
Gender (male)	1.595 (1.022, 2.490)	0.040	0.806 (0.490, 1.326)	0.396
BMI (kg/m ²)	0.975 (0.914, 1.039)	0.432		
Current smoking	2.213 (1.197, 4.089)	0.011	1.601 (0.818, 3.134)	0.169
Drinking	1.892 (0.823, 4.350)	0.133		
Hypertension	1.086 (0.696, 1.697)	0.715		
Hyperglycaemia	0.772 (0.484, 1.233)	0.279		
Hyperlipidemia	0.845 (0.541, 1.320)	0.459		
Urea (mmol/L)	0.974 (0.873, 1.085)	0.629		
CREA (μmol/L)	1.002 (0.993, 1.011)	0.656		
Urea/CREA	0.739 (0.128, 4.267)	0.735		
UA (μmol/L)	0.997 (0.995, 1.000)	0.041	0.998 (0.996, 1.001)	0.185
COPD	0.977 (0.618, 1.547)	0.923		
TIA/stroke/embolism	0.972 (0.592, 1.594)	0.909		
CHA ₂ DS ₂ -VaSc score	1.070 (0.930, 1.231)	0.343		
EHRA classification				
EHRA 1	0.634 (0.295, 1.363)	0.243		
EHRA 2a	1.112 (0.741, 1.669)	0.607		
EHRA 2b	1.231 (0.835, 1.813)	0.294		
EHRA 3	0 (Ref)			
WBC (10 ⁹ /L)	0.981 (0.885, 1.088)	0.718		
NE (10 ⁹ /L)	0.975 (0.872, 1.090)	0.657		
LY (10 ⁹ /L)	1.103 (0.752, 1.618)	0.616		
MO (10 ⁹ /L)	0.679 (0.199, 2.316)	0.536		
PLT (10 ⁹ /L)	1.000 (0.997, 1.004)	0.764		
NLR	0.962 (0.874, 1.057)	0.418		
PLR	0.999 (0.996, 1.002)	0.691		
LMR	1.079 (0.953, 1.222)	0.232		
SII	1.000 (1.000, 1.000)	0.573		
CAD	1.340 (0.840, 2.137)	0.219		
LA diameter (mm)	0.998 (0.966, 1.030)	0.883		
LA circumference (mm)	0.998 (0.992, 1.003)	0.342		
LA square (mm ²)	1.000 (1.000, 1.000)	0.332		
LA-FD	24.310 (9.740, 60.671)	<0.001	21.750 (8.533, 55.444)	<0.001

AF, atrial fibrillation; BMI, body mass index; CI, confidence interval; CREA, creatinine; COPD, chronic obstructive pulmonary disease; CAD, coronary artery disease; EHRA, European Heart Rhythm Association; FD, fractal dimension; HR, hazard ratio; LY, lymphocyte count; LMR, lymphocyte-to-monocyte ratio; LA, left atrium; MO, monocyte count; NE, neutrophil count; NLR, neutrophil-to-lymphocyte ratio; PLT, platelet count; PLR, platelet-to-lymphocyte ratio; SII, systemic immune-inflammation index [(neutrophil count × platelet count)/lymphocyte count]; TIA, transient ischemic attack; UA, uric acid; WBC, white blood cell count.

Table 4 Cox regression analysis for AF recurrence in patients with persistent AF

Parameters	Univariate Cox regression		Multivariate Cox regression	
	HR (95% CI)	P value	HR (95% CI)	P value
Age (years)	0.990 (0.968, 1.013)	0.389		
Gender (male)	0.895 (0.520, 1.541)	0.689		
BMI (kg/m ²)	1.030 (0.971, 1.092)	0.322		
Current smoking	1.294 (0.716, 2.338)	0.393		
Drinking	1.163 (0.633, 2.137)	0.626		
Hypertension	1.085 (0.666, 1.767)	0.744		
Hyperglycaemia	0.756 (0.451, 1.268)	0.290		
Hyperlipidemia	0.986 (0.603, 1.612)	0.954		
Urea (mmol/L)	0.947 (0.837, 1.070)	0.379		
CREA (μmol/L)	1.001 (0.992, 1.010)	0.848		
Urea/CREA	0.171 (0.000, 1,209.035)	0.696		
UA (μmol/L)	1.000 (0.998, 1.002)	0.997		
COPD	1.010 (0.612, 1.666)	0.969		
TIA/stroke/embolism	0.550 (0.335, 0.903)	0.018	0.597 (0.363, 0.982)	0.042
CHA ₂ DS ₂ -VaSc score	1.036 (0.873, 1.230)	0.683		
EHRA classification				
EHRA 1	1.120 (0.365, 3.441)	0.843		
EHRA 2a	1.102 (0.552, 2.203)	0.782		
EHRA 2b	1.439 (0.741, 2.793)	0.282		
EHRA 3	0 (Ref)			
WBC (10 ⁹ /L)	0.954 (0.840, 1.083)	0.464		
NE (10 ⁹ /L)	0.963 (0.839, 1.105)	0.588		
LY (10 ⁹ /L)	0.785 (0.523, 1.179)	0.243		
MO (10 ⁹ /L)	1.797 (0.450, 7.183)	0.407		
PLT (10 ⁹ /L)	1.000 (0.996, 1.004)	0.980		
NLR	1.012 (0.920, 1.114)	0.800		
PLR	1.002 (0.997, 1.007)	0.521		
LMR	0.867 (0.742, 1.013)	0.073		
SII	1.000 (1.000, 1.001)	0.632		
CAD	1.176 (0.718, 1.926)	0.520		
LA diameter (mm)	0.991 (0.955, 1.027)	0.609		
LA circumference (mm)	0.996 (0.990, 1.002)	0.198		
LA square (mm ²)	1.000 (1.000, 1.000)	0.498		
LA-FD	8.454 (2.316, 30.864)	0.001	7.291 (1.977, 26.896)	0.003

AF, atrial fibrillation; BMI, body mass index; CI, confidence interval; CREA, creatinine; COPD, chronic obstructive pulmonary disease; CAD, coronary artery disease; EHRA, European Heart Rhythm Association; FD, fractal dimension; HR, hazard ratio; LY, lymphocyte count; LMR, lymphocyte-to-monocyte ratio; LA, left atrium; MO, monocyte count; NE, neutrophil count; NLR, neutrophil-to-lymphocyte ratio; PLT, platelet count; PLR, platelet-to-lymphocyte ratio; SII, systemic immune-inflammation index [(neutrophil count × platelet count)/lymphocyte count; TIA, transient ischemic attack; UA, uric acid; WBC, white blood cell count.

Other clinical characteristics such as sex and age did not predict non-improvement in EHRA symptom scores (Table 5). The findings of the multivariate Cox regression analysis suggested that LA-FD (HR =10.500, 95% CI: 3.086–35.728, $P<0.001$) was an independent predictor of non-improvement in EHRA symptom scores (Table 5). Kaplan-Meier survival curves suggested a lower incidence of EHRA symptom score improvement in patients with a larger LA-FD (>1.208) than in those with a smaller LA-FD (<1.208) (Figure 3D).

Discussion

The aim of the present study was to investigate the relationship between LA-FD and recurrence after ablation for AF and to determine whether the EHRA symptom score improves after treatment. The FD can be used as a quantitative marker to characterize LA morphology and has been used to assess several cardiovascular diseases (13,14). The main finding of the present study was that LA-FD was an independent predictor of recurrence and non-improvement in EHRA symptom scores after AF ablation. In addition, patients with a larger LA-FD (>1.208) had a higher incidence of recurrent AF and no improvement in the EHRA symptom scores than those with a smaller LA-FD (<1.208).

The LA is recognized as an indicator of adverse cardiovascular outcomes, particularly the occurrence, progression, and prognosis of AF (15-17). LA remodeling is a crucial factor that contributes to recurrence after AF ablation (7,18). LA remodeling includes neural, electrical, and structural remodeling, and its structural remodeling is characterized by changes in LA size parameters detectable by imaging (19,20). A retrospective study found that the ratio of the larger box lesion surface area to the total LA surface area was protective against recurrence after persistent AF ablation (21). Wang *et al.* (22) showed that both larger and smaller LA diameters and an ellipsoidal model/body surface area were associated with a higher risk of AF recurrence one year after radiofrequency ablation. Chollet *et al.* (23) found that an LA volume index ≥ 42 mL/m² was an independent predictor of recurrence 1 year after pulmonary vein isolation in patients with AF. A meta-analysis suggested that a larger LA volume/volume index increases the risk of AF recurrence after radiofrequency ablation (24). Thus, LA remodeling is an established cause of recurrence after AF ablation and can be clinically monitored by imaging.

Currently, LA remodeling is characterized by its morphological features (25,26). Shi *et al.* (25) demonstrated that the LA sphericity index was an independent predictor of AF recurrence following radiofrequency ablation. Nedios *et al.* (26) reported a higher LA asymmetry index after ablation in patients with AF recurrence than in those without recurrence. A study of two cohorts showed that fractal LA measurements on CT images were related to AF recurrence after ablation (27). In addition, Bisbal *et al.* (7) determined that LA sphericity quantified using a 3D model of the LA chamber is one of the strongest predictors of recurrence after AF ablation. In the current study, we found that FD, as a quantitative characterization of LA morphologic heterogeneity, was significantly correlated with AF ablation outcomes, and that a high FD predicted a higher rate of postprocedural recurrence. This may be explained by the fact that a larger FD indicates poor structural remodeling of the LA, which promotes electrical remodeling and creates a favorable environment for the development of AF.

Another important aspect confirmed in this study is that LA-FD was also associated with no improvement in EHRA symptom scores. This was predictable because patients with non-improvement in EHRA symptom scores usually have a poorer clinical prognosis, which may be closely related to adverse LA remodeling (15,28). Moreover, we observed that AF type was a clinically valid predictor of AF recurrence after ablation, which is consistent with previous studies (29,30). Interestingly, we stratified patients with AF and showed that a high LA-FD was associated with a higher rate of postoperative AF recurrence, both in patients with paroxysmal and those with persistent AF. Therefore, FD can be used as an indicator for the preoperative evaluation of AF ablation in the clinic, thereby helping to select the patients who will have the optimum benefit from the procedure.

Recent artificial intelligence (AI)-enabled LA volumetry techniques have demonstrated high predictive accuracy for AF and stroke (31-33). However, our findings suggest that FD analysis captures finer morphological details that are not reflected in volume-based assessments. While AI volumetry offers rapid and automated analysis, FD provides unique insights into atrial morphology, offering potential for early detection of atrial remodeling and fibrosis. Integrating FD with AI volumetry could provide a more comprehensive evaluation of atrial remodeling, aiding in personalized risk stratification.

Previous studies have shown that AF is more prevalent in males than females, which could account for the higher

Table 5 Cox regression analysis for EHRA symptom score non-improvement

Parameters	Univariate Cox regression		Multivariate Cox regression	
	HR (95% CI)	P value	HR (95% CI)	P value
Age (years)	0.984 (0.967, 1.001)	0.065		
Gender (male)	1.334 (0.875, 2.034)	0.180		
BMI (kg/m ²)	0.990 (0.932, 1.051)	0.747		
Current smoking	0.781 (0.467, 1.308)	0.348		
Drinking	0.879 (0.479, 1.613)	0.677		
Hypertension	1.234 (0.824, 1.847)	0.308		
Hyperglycaemia	1.013 (0.662, 1.550)	0.953		
Hyperlipidemia	0.629 (0.416, 0.952)	0.028	0.707 (0.456, 1.095)	0.121
Urea (mmol/L)	0.960 (0.871, 1.059)	0.414		
CREA (μmol/L)	1.002 (0.996, 1.008)	0.560		
Urea/CREA	0.250 (0.000, 293.268)	0.701		
UA (μmol/L)	0.998 (0.997, 1.000)	0.132		
COPD	1.240 (0.822, 1.871)	0.305		
TIA/stroke/embolism	1.066 (0.687, 1.654)	0.775		
Type of AF	0.980 (0.649, 1.481)	0.924		
CHA ₂ DS ₂ -VaSc score	0.911 (0.799, 1.038)	0.163		
EHRA classification				
EHRA 1	0.820 (0.307, 2.190)	0.692		
EHRA 2a	1.306 (0.705, 2.416)	0.396		
EHRA 2b	1.051 (0.568, 1.943)	0.875		
EHRA 3	0 (Ref)			
WBC (10 ⁹ /L)	1.003 (0.918, 1.095)	0.954		
NE (10 ⁹ /L)	0.966 (0.875, 1.068)	0.503		
LY (10 ⁹ /L)	1.484 (1.097, 2.007)	0.010	1.095 (0.706, 1.697)	0.686
MO (10 ⁹ /L)	1.227 (0.441, 3.416)	0.695		
PLT (10 ⁹ /L)	1.003 (1.001, 1.006)	0.013	1.002 (0.999, 1.005)	0.126
NLR	0.910 (0.836, 0.990)	0.029	0.918 (0.828, 1.019)	0.107
PLR	0.999 (0.995, 1.002)	0.382		
LMR	1.107 (0.988, 1.240)	0.080		
SII	1.000 (0.999, 1.000)	0.279		
CAD	1.408 (0.922, 2.150)	0.113		
LA diameter (mm)	0.995 (0.964, 1.027)	0.746		
LA circumference (mm)	0.997 (0.993, 1.002)	0.224		
LA square (mm ²)	1.000 (1.000, 1.000)	0.287		
LA-FD	7.555 (2.347, 24.323)	0.001	10.500 (3.086, 35.728)	<0.001

AF, atrial fibrillation; BMI, body mass index; CI, confidence interval; CREA, creatinine; COPD, chronic obstructive pulmonary disease; CAD, coronary artery disease; EHRA, European Heart Rhythm Association; FD, fractal dimension; HR, hazard ratio; LY, lymphocyte count; LMR, lymphocyte-to-monocyte ratio; LA, left atrium; MO, monocyte count; NE, neutrophil count; NLR, neutrophil-to-lymphocyte ratio; PLT, platelet count; PLR, platelet-to-lymphocyte ratio; SII, systemic immune-inflammation index [(neutrophil count × platelet count)/lymphocyte count]; TIA, transient ischemic attack; UA, uric acid; WBC, white blood cell count.

proportion of male patients in this study cohort (34,35). The lack of significant gender differences in AF recurrence and symptom improvement may also be explained by the fact that structural remodeling in the left atrium, such as changes in LA morphology and size, may affect both male and female patients similarly. Nonetheless, gender-related factors such as hormonal differences and comorbidities could still play a role in long-term outcomes, and further studies with larger cohorts and longer follow-up periods are warranted to investigate these potential differences in greater depth.

This study had some limitations. First, this was designed as a single-center retrospective study, and some patients with incomplete information or those lost to follow-up were excluded, which may have led to selection bias. In contrast, follow-up was prospective and meaningful. Second, the morphological heterogeneity of the LA, except for quantification by FD, should be explored to determine the correlation between additional morphological indicators and AF recurrence. Finally, in addition to AF recurrence, the prognostic value of LA-FD may be applied to other cardiac conditions, warranting further exploration.

Conclusions

In conclusion, a larger LA-FD (>1.208) on cardiac CTA images is an indication of adverse LA remodeling and an independent predictor of recurrence and non-improvement in the EHRA symptom score after ablation for AF.

Acknowledgments

The abstract of this manuscript has been accepted for presentation as an oral paper presentation at the 110th Scientific Assembly and Annual Meeting of the Radiological Society of North America (Session Number: T7-SSCA06).

Footnote

Reporting Checklist: The authors have completed the STROBE reporting checklist. Available at <https://qims.amegroups.com/article/view/10.21037/qims-24-2049/rc>

Funding: This work was supported by the National Natural Science Foundation of China (grant No. 82371914 to J.Z.), and Medical Innovation and Development Project of Lanzhou University (No. lzuyxcx-2022-139 to J.Z.).

Conflicts of Interest: All authors have completed the ICMJE uniform disclosure form (available at <https://qims.amegroups.com/article/view/10.21037/qims-24-2049/coif>). W.R. reports that he is an Employee of GE Healthcare, the manufacturer of the CT scanner used in this study. J.Z. reports that this work was supported by the National Natural Science Foundation of China (grant No. 82371914), and Medical Innovation and Development Project of Lanzhou University (No. lzuyxcx-2022-139). The other authors have no conflicts of interest to declare.

Ethical Statement: The authors are accountable for all aspects of the work in ensuring that questions related to the accuracy or integrity of any part of the work are appropriately investigated and resolved. This study was conducted in accordance with the Declaration of Helsinki (as revised in 2013). The Ethics Committee of the Lanzhou University Second Hospital approved this study (ethical board approval number: 2023A-702). The informed consent was exempted for all individual patients because of the retrospective nature of the study.

Open Access Statement: This is an Open Access article distributed in accordance with the Creative Commons Attribution-NonCommercial-NoDerivs 4.0 International License (CC BY-NC-ND 4.0), which permits the non-commercial replication and distribution of the article with the strict proviso that no changes or edits are made and the original work is properly cited (including links to both the formal publication through the relevant DOI and the license). See: <https://creativecommons.org/licenses/by-nc-nd/4.0/>.

References

1. Sagris M, Vardas EP, Theofilis P, Antonopoulos AS, Oikonomou E, Tousoulis D. Atrial Fibrillation: Pathogenesis, Predisposing Factors, and Genetics. *Int J Mol Sci* 2021;23:6.
2. Brundel BJM, Ai X, Hills MT, Kuipers MF, Lip GYH, de Groot NMS. Atrial fibrillation. *Nat Rev Dis Primers* 2022;8:21.
3. Hindricks G, Potpara T, Dagres N, Arbelo E, Bax JJ, Blomström-Lundqvist C, et al. 2020 ESC Guidelines for the diagnosis and management of atrial fibrillation developed in collaboration with the European Association for Cardio-Thoracic Surgery (EACTS): The Task Force for the diagnosis and management of atrial fibrillation of

- the European Society of Cardiology (ESC) Developed with the special contribution of the European Heart Rhythm Association (EHRA) of the ESC. *Eur Heart J* 2021;42:373-498.
4. January CT, Wann LS, Calkins H, Chen LY, Cigarroa JE, Cleveland JC Jr, Ellinor PT, Ezekowitz MD, Field ME, Furie KL, Heidenreich PA, Murray KT, Shea JB, Tracy CM, Yancy CW. 2019 AHA/ACC/HRS Focused Update of the 2014 AHA/ACC/HRS Guideline for the Management of Patients With Atrial Fibrillation: A Report of the American College of Cardiology/American Heart Association Task Force on Clinical Practice Guidelines and the Heart Rhythm Society. *J Am Coll Cardiol* 2019;74:104-32.
 5. Kirchhof P, Benussi S, Kotecha D, Ahlsson A, Atar D, Casadei B, et al. 2016 ESC Guidelines for the management of atrial fibrillation developed in collaboration with EACTS. *Europace* 2016;18:1609-78.
 6. Kocyigit D, Yalcin MU, Gurses KM, Turk G, Ardali S, Canpolat U, Evranos B, Yorgun H, Hazirolan T, Aytemir K. Impact of anatomical features of the left atrial appendage on outcomes after cryoablation for atrial fibrillation. *J Cardiovasc Comput Tomogr* 2019;13:105-12.
 7. Bisbal F, Alarcón F, Ferrero-de-Loma-Orsio A, González-Ferrer JJ, Alonso C, Pachón M, Tizón H, Cabanas-Grandío P, Sanchez M, Benito E, Teis A, Ruiz-Granell R, Pérez-Villacastín J, Viñolas X, Arias MA, Vallés E, García-Campo E, Fernández-Lozano I, Villuendas R, Mont L. Left atrial geometry and outcome of atrial fibrillation ablation: results from the multicentre LAGO-AF study. *Eur Heart J Cardiovasc Imaging* 2018;19:1002-9.
 8. Straube F, Pongratz J, Hartl S, Brueck B, Tesche C, Ebersberger U, Helmberger T, Crispin A, Wankerl M, Dorwarth U, Hoffmann E. Cardiac computed tomography angiography-derived analysis of left atrial appendage morphology and left atrial dimensions for the prediction of atrial fibrillation recurrence after pulmonary vein isolation. *Clin Cardiol* 2021;44:1636-45.
 9. Strisciuglio T, Di Gioia G, Chatzikiyriakou S, Silva Garcia E, Barbato E, Geelen P, De Potter T. Left atrial volume computed by 3D rotational angiography best predicts atrial fibrillation recurrence after circumferential pulmonary vein isolation. *Int J Cardiovasc Imaging* 2018;34:337-42.
 10. Lennon FE, Cianci GC, Cipriani NA, Hensing TA, Zhang HJ, Chen CT, Murgu SD, Vokes EE, Vannier MW, Salgia R. Lung cancer-a fractal viewpoint. *Nat Rev Clin Oncol* 2015;12:664-75.
 11. Ghatak S, Chakraborti S, Gupta M, Dutta S, Pati SK, Bhattacharya A. Fractal Dimension-Based Infection Detection in Chest X-ray Images. *Appl Biochem Biotechnol* 2023;195:2196-215.
 12. Torres Hoyos F, Navarro RB, Vergara Villadiego J, Guerrero-Martelo M. Geometrical study of astrocytomas through fractals and scaling analysis. *Appl Radiat Isot* 2018;141:250-6.
 13. Yu S, Chen X, Yang K, Wang J, Zhao K, Dong W, Yan W, Su G, Zhao S. Correlation between left ventricular fractal dimension and impaired strain assessed by cardiac MRI feature tracking in patients with left ventricular noncompaction and normal left ventricular ejection fraction. *Eur Radiol* 2022;32:2594-603.
 14. Captur G, Lopes LR, Patel V, Li C, Bassett P, Syrris P, Sado DM, Maestrini V, Mohun TJ, McKenna WJ, Muthurangu V, Elliott PM, Moon JC. Abnormal cardiac formation in hypertrophic cardiomyopathy: fractal analysis of trabeculae and preclinical gene expression. *Circ Cardiovasc Genet* 2014;7:241-8.
 15. Thomas L, Abhayaratna WP. Left Atrial Reverse Remodeling: Mechanisms, Evaluation, and Clinical Significance. *JACC Cardiovasc Imaging* 2017;10:65-77.
 16. Khan HR, Yakupoglu HY, Kralj-Hans I, Halder S, Bahrami T, Clague J, De Souza A, Hussain W, Jarman J, Jones DG, Salukhe T, Markides V, Gupta D, Khattar R, Wong T; ClinicalService 1STOP Project Investigators. Left Atrial Function Predicts Atrial Arrhythmia Recurrence Following Ablation of Long-Standing Persistent Atrial Fibrillation. *Circ Cardiovasc Imaging* 2023;16:e015352.
 17. Assaf A, Mekhael M, Noujaim C, Chouman N, Younes H, Feng H, ElHajjar A, Shan B, Kistler P, Kreidieh O, Marrouche N, Donnellan E. Effect of fibrosis regionality on atrial fibrillation recurrence: insights from DECAAF II. *Europace* 2023;25:euad199.
 18. Beyer C, Tokarska L, Stühlinger M, Feuchtner G, Hintringer F, Honold S, Fiedler L, Schönbauer MS, Schönbauer R, Plank F. Structural Cardiac Remodeling in Atrial Fibrillation. *JACC Cardiovasc Imaging* 2021;14:2199-208.
 19. Nattel S, Harada M. Atrial remodeling and atrial fibrillation: recent advances and translational perspectives. *J Am Coll Cardiol* 2014;63:2335-45.
 20. Tondo C, Iacopino S, Pieragnoli P, Molon G, Verlato R, Curnis A, Landolina M, Allocca G, Arena G, Fassini G, Sciarra L, Luzi M, Manfrin M, Padeletti L; ClinicalService 1STOP Project Investigators. Pulmonary vein isolation cryoablation for patients with persistent and long-standing persistent atrial fibrillation: Clinical outcomes from

- the real-world multicenter observational project. *Heart Rhythm* 2018;15:363-8.
21. Keçe F, Scholte AJ, de Riva M, Naruse Y, Watanabe M, Alizadeh Dehnavi R, Schali J MJ, Zeppenfeld K, Trines SA. Impact of left atrial box surface ratio on the recurrence after ablation for persistent atrial fibrillation. *Pacing Clin Electrophysiol* 2019;42:208-15.
 22. Wang Q, Zhuo C, Shang Y, Zhao J, Chen N, Lv N, Huang Y, Zheng L, Lai J, Han J, Shu Z. U-Shaped Relationship Between Left Atrium Size on Echocardiography and 1-Year Recurrence of Atrial Fibrillation After Radiofrequency Catheter Ablation - Prognostic Value Study. *Circ J* 2019;83:1463-71.
 23. Chollet L, Iqbal SUR, Wittmer S, Thalmann G, Madaffari A, Kozhuharov N, Galuszka O, Küffer T, Gräni C, Brugger N, Servatius H, Noti F, Haeberlin A, Roten L, Tanner H, Reichlin T. Impact of atrial fibrillation phenotype and left atrial volume on outcome after pulmonary vein isolation. *Europace* 2024;26:euae071.
 24. Njoku A, Kannabhiran M, Arora R, Reddy P, Gopinathannair R, Lakkireddy D, Dominic P. Left atrial volume predicts atrial fibrillation recurrence after radiofrequency ablation: a meta-analysis. *Europace* 2018;20:33-42.
 25. Shi J, Xu S, Chen L, Wu B, Yang K, Chen S, Zhou D, Zhang B, Xuan T, Hu X. Impact of Left Atrial Sphericity Index on the Outcome of Catheter Ablation for Atrial Fibrillation. *J Cardiovasc Transl Res* 2021;14:912-20.
 26. Nedios S, Koutalas E, Sommer P, Arya A, Rolf S, Husser D, Bollmann A, Hindricks G, Breithardt OA. Asymmetrical left atrial remodelling in atrial fibrillation: relation with diastolic dysfunction and long-term ablation outcomes. *Europace* 2017;19:1463-9.
 27. Firouznia M, Feeny AK, LaBarbera MA, McHale M, Cantlay C, Kalfas N, Schoenhagen P, Saliba W, Tchou P, Barnard J, Chung MK, Madabhushi A. Machine Learning-Derived Fractal Features of Shape and Texture of the Left Atrium and Pulmonary Veins From Cardiac Computed Tomography Scans Are Associated With Risk of Recurrence of Atrial Fibrillation Postablation. *Circ Arrhythm Electrophysiol* 2021;14:e009265.
 28. Freeman JV, Simon DN, Go AS, Spertus J, Fonarow GC, Gersh BJ, Hylek EM, Kowey PR, Mahaffey KW, Thomas LE, Chang P, Peterson ED, Piccini JP; Outcomes Registry for Better Informed Treatment of Atrial Fibrillation (ORBIT-AF) Investigators and Patients. Association Between Atrial Fibrillation Symptoms, Quality of Life, and Patient Outcomes: Results From the Outcomes Registry for Better Informed Treatment of Atrial Fibrillation (ORBIT-AF). *Circ Cardiovasc Qual Outcomes* 2015;8:393-402.
 29. Pathak RK, Middeldorp ME, Lau DH, Mehta AB, Mahajan R, Twomey D, Alasady M, Hanley L, Antic NA, McEvoy RD, Kalman JM, Abhayaratna WP, Sanders P. Aggressive risk factor reduction study for atrial fibrillation and implications for the outcome of ablation: the ARREST-AF cohort study. *J Am Coll Cardiol* 2014;64:2222-31.
 30. Calkins H, Hindricks G, Cappato R, Kim YH, Saad EB, Aguinaga L, et al. 2017 HRS/EHRA/ECAS/APHRS/SOLAECE expert consensus statement on catheter and surgical ablation of atrial fibrillation. *Heart Rhythm* 2017;14:e275-444.
 31. Naghavi M, Reeves A, Budoff M, Li D, Atlas K, Zhang C, Atlas T, Roy SK, Henschke CI, Wong ND, Defilippi C, Levy D, Yankelevitz DF. AI-enabled cardiac chambers volumetry in coronary artery calcium scans (AI-CAC(TM)) predicts heart failure and outperforms NT-proBNP: The multi-ethnic study of Atherosclerosis. *J Cardiovasc Comput Tomogr* 2024;18:392-400.
 32. Onnis C, van Assen M. New Frontiers for Predicting Atrial Fibrillation and Stroke: AI-Based Left Atrial Volumetry. *JACC Adv* 2024;3:101299.
 33. Naghavi M, Reeves AP, Atlas KC, Zhang C, Li D, Atlas T, Henschke CI, Wong ND, Roy SK, Budoff MJ, Yankelevitz DF. AI-Enabled CT Cardiac Chamber Volumetry Predicts Atrial Fibrillation and Stroke Comparable to MRI. *JACC Adv* 2024;3:101300.
 34. Du X, Guo L, Xia S, Du J, Anderson C, Arima H, Huffman M, Yuan Y, Zheng Y, Wu S, Guang X, Zhou X, Lin H, Cheng X, Dong J, Ma C. Atrial fibrillation prevalence, awareness and management in a nationwide survey of adults in China. *Heart* 2021. [Epub ahead of print]. doi: 10.1136/heartjnl-2020-317915.
 35. Shi S, Tang Y, Zhao Q, Yan H, Yu B, Zheng Q, et al. Prevalence and risk of atrial fibrillation in China: A national cross-sectional epidemiological study. *Lancet Reg Health West Pac* 2022;23:100439.
- Cite this article as:** Jing M, Liu Q, Xi H, Yang X, Zhu H, Sun Q, Chen G, Zhang Y, Ren W, Deng L, Han T, Zhang B, Zhou J. Recurrence and non-improvement of European Heart Rhythm Association symptom scores after atrial fibrillation ablation: the role of left atrial fractal dimension. *Quant Imaging Med Surg* 2025;15(4):3602-3615. doi: 10.21037/qims-24-2049